



Contents lists available at ScienceDirect

Chinese Chemical Letters

journal homepage: www.elsevier.com/locate/ccllet

Research advances of tetrahedral framework nucleic acid-based systems in biomedicine

Lihang Wang^a, Mary Li Javier^b, Chunshan Luo^a, Tingsheng Lu^a, Shudan Yao^a, Bing Qiu^{a,*}, Yun Wang^{b,*}, Yunfeng Lin^{b,c,*}

^a Department of Spine Surgery, Beijing Jishuitan Hospital Guizhou Hospital, Guiyang 550014, China

^b State Key Laboratory of Oral Diseases, National Center for Stomatology, National Clinical Research Centre for Oral Diseases, West China Hospital of Stomatology, Sichuan University, Chengdu 610041, China

^c Sichuan Provincial Engineering Research Center of Oral Biomaterials, Chengdu 610041, China

ARTICLE INFO

Article history:

Received 10 December 2023

Revised 30 January 2024

Accepted 31 January 2024

Available online 2 February 2024

Keywords:

DNA nanomaterials

Tetrahedral framework nucleic acid

Drug delivery

Antioxidation

Immunomodulation

Tissue regeneration

Antitumor therapy

ABSTRACT

This article reviews the latest research advances of tetrahedral framework nucleic acid (tFNA)-based systems in their fabrication, modification, and the potential applications in biomedicine. TFNA arises from the synthesis of four single-stranded DNA chains. Each chain contains brief sequences that complement those found in the other three, culminating in the creation of a pyramid-shaped nanostructure of approximately 10 nanometers in size. The first generation of tFNA demonstrates inherent compatibility with biological systems and the ability to permeate cell membrane effectively. These attributes translate into remarkable capabilities for regulating various cellular biological processes, fostering tissue regeneration, and modulating immune responses. The subsequent evolution of tFNA introduces enhanced adaptability and a relatively higher degree of biological stability. This advancement encompasses structural modifications, such as the addition of functional domains at the vertices or side arms, integration of low molecular weight pharmaceuticals, and the implementation of diverse strategies aimed at reversing multi-drug resistance in tumor cells or microorganisms. These augmentations empower tFNA-based systems to be utilized in different scenarios, thus broadening their potential applications in various biomedical fields.

© 2024 Published by Elsevier B.V. on behalf of Chinese Chemical Society and Institute of Materia Medica, Chinese Academy of Medical Sciences.

1. Introduction

Deoxyribonucleic acid (DNA) is a molecular structure that stores Genetic information within living organisms. It consists of a double helical structure composed of base pairs and a pentose-phosphate backbone. Widely present in living organisms, DNA is composed of numerous nucleotides, each consisting of a pentose molecule, a base, and a phosphate group. The pentose molecule and phosphate group form the backbone, with phosphates connecting with adjacent pentose molecules to create a chain-like structure. Bases are linked to pentose molecules *via* N-glycosidic bonds. Two chains are connected by base pairs with a pairing strategy known as complementary base pairing, arranged in a reverse direction to form a helical double-stranded structure. This structure is not only stable but also serves the crucial function of replicating and transmitting genetic information, making it a fundamental molecule in biology [1–4].

Professor Nedrian Seeman established a groundbreaking research domain in DNA nanotechnology by spearheading the application of DNA sequences in structural construction [2]. Over recent years, DNA nanostructures have garnered widespread adoption across a spectrum of disciplines. Their outstanding adaptability provides an unparalleled level of precision at the nanoscale, endowing them with immense value as tools in numerous sectors, spanning bioimaging, biocomputing, biomimetic structure development, and drug delivery applications [5,6]. The comprehensive physical and chemical attributes inherent in DNA structures, encompassing their physical configuration, dimensions, charge, and nucleic acid composition, bestow upon them the capability to execute a myriad of functions. The simplicity of synthesis, high yield, and cost-effectiveness has propelled tetrahedral framework nucleic acids (tFNA) as a widely applied DNA nanostructure. Lin and his colleagues have extensively employed tFNA in various disease models. *In-vivo* experiments have demonstrated the ability of tFNA to intervene to varying extents in the onset and progression of diverse diseases [6]. Remarkably, this material exhibits exceptional anti-inflammatory and antioxidant capabilities, thereby ameliorating pathological phenotypes associated with inflammation such

* Corresponding authors.

E-mail addresses: yz8088gk@163.com (B. Qiu), wy630ivy@outlook.com (Y. Wang), yunfenglin@scu.edu.cn (Y. Lin).

as skin damage, osteoarthritis, and acute kidney injury [7–11]. Furthermore, previous research has revealed that tFNA contributes to cell proliferation, migration, autophagy, and the maintenance of stemness in stem cells [12,13].

Currently, tFNA can be categorized into three generations based on their development timeline. The first generation comprises pure tFNA with only a tetrahedral framework structure, which is primarily used to regulate cell behavior, promote tissue regeneration, and modulate the immune system. The second generation involves tFNA-based functional systems, utilizing this tetrahedral framework for the transport of RNA, peptides, and small-molecule drugs through physical or chemical means, aiming at targeted therapy, anticancer and antimicrobial treatment for the purpose of overcoming drug resistance. The third generation consists of structure-controlled tFNA, designed with conditional switches in the assembly process for precise drug release based on stimulus-responsive mechanisms. This article will primarily discuss the functional systems of the first and second generations of tFNA.

2. Design tools for DNA nanostructures and the discovery of tFNA

Douglas presented findings on caDNAno, an open-source software package crucial for designing the scale of double helices and their chiral rotations in DNA molecules. This tool has played a pivotal role in formulating DNA sequences for constructing intricate 3D honeycomb-folded shapes [14]. Tiamat, distinguished as a three-dimensional DNA editing tool, is dedicated to shaping the topological structure and complementary pairing relationships within DNA [15]. The utilization of Cando and oxDNA has been instrumental in both designing DNA structures and performing quasi-molecular dynamics analyses [16,17]. A recent addition to the toolkit, MagicDNA, proposed by Castro's team, boasts an integrated suite of functionalities and a user-friendly visual interface [18]. In concert, these tools empower the generation of diverse DNA architectures. This encompasses the folding of lengthy single-stranded DNA (ssDNA) with short ssDNA molecules, resulting in the creation of DNA origami structures [19]. Additionally, the folding of a sequence of short ssDNA molecules is employed to construct DNA frameworks [20], while the assembly of expansive two-dimensional or three-dimensional DNA arrays relies on self-assembling DNA fragments [21]. It was discovered that four 63-nt-long ssDNAs, each with a GC content of approximately 50%, hybridize to form a pyramid-shaped tetrahedral nanostructure of about 10 nanometers in size. This structure minimizes the free energy of ssDNA, has minimal formation of secondary structures, and is the most stable minimal-size DNA nanostructure in three dimensions. These four ssDNAs complement each other, folding into triangular blocks with edges of 20 base pairs, and each vertex has a nucleotide to assist in folding. It was further found that this structure has significant biological functions and applications.

3. Characterization of tFNA

The effective synthesis of tFNA is validated through various characterization techniques [11]. Molecular weights of single-stranded DNA, tFNA, and nucleic acids loaded onto tFNA (such as those linked with adapters or microRNA-tFNA) are observed using high-performance capillary electrophoresis (HPCE) and polyacrylamide gel electrophoresis (PAGE). Transmission electron microscopy (TEM) and atomic force microscopy (AFM) provide insights into the conical cube structure and spatial size of tFNA. Dynamic light scattering (DLS) is used to assess the distribution of zeta potential and hydrodynamic size of both tFNA and their functional systems in water. Furthermore, high-performance liquid

chromatography (HPLC) is utilized to determine the optimal efficiency of drug loading.

4. Functional tFNA with oligonucleotides

The advancement in single-stranded DNA chemical synthesis has facilitated the attachment of DNA aptamers, microRNAs, or other oligonucleotides to one end of a single strand. In 2011, it was discovered that tetrahedral framework nucleic acid structures could effectively carry CpG oligonucleotides. Owing to their spatial stability and cell membrane permeability, this compound body was taken up non-invasively by macrophage-like RAW264.7 cells [22]. To mitigate interference from structure formation and ensure the complete release of functional domains, a typical approach involves using 4–5 nucleotides A or T to link the oligonucleotide and single-stranded DNA [23]. Post-assembly, the oligonucleotide is attached to one or more vertices of tFNA.

The tFNA-based delivery system serves a dual purpose. Firstly, it enhances the biological stability of single-stranded DNA, microRNA, and other short nucleic acids in challenging environments like fetal bovine serum, enzyme-containing solutions, and the body fluids of living animals. Secondly, tFNA promotes functional biological materials to permeate into cells. Oligonucleotides can be linked to tFNA vertices or side arms using either direct attachment or sticky-end hybridization, depending on the payload and synthesis technique [24]. For easily degradable molecules like miRNA, the latter sticky-end hybridization modification method is recommended to prevent unexpected degradation. Extending the tFNA structure through sticky-end hybridization is a commonly employed method, leading to the successful development of multiple tFNA functional systems widely applied in areas such as immune regulation, tumor suppression, tissue regeneration, and induction of stem cells [23].

5. Functional tFNA for delivering small molecular weight drugs

The growing interest in the immunomodulatory potential of traditional Chinese medicine (TCM) has led to increased research efforts. Nevertheless, obstacles such as inadequate water solubility, short biological half-life, and constrained biological stability in both local and systemic applications have spurred the exploration of inventive remedies. In response, we have designed and implemented several tetrahedral framework nucleic acid (tFNA)-based delivery systems for TCM. The primary objective of these systems is to facilitate the incorporation of TCM monomers into target cells, thereby imposing a synergistic effect. By leveraging the unique properties of tFNA, including spatial stability and enhanced cell membrane permeability, we aim to address the limitations associated with traditional TCM administration. This novel approach holds promise for improving the water solubility, extending the biological half-life, and enhancing the overall biological stability of TCM compounds. Through the strategic construction of tFNA-based delivery systems, we anticipate overcoming key obstacles associated with TCM application, particularly in the context of modulating immune responses. This innovative method not only enhances the delivery efficiency of TCM monomers but also opens new avenues for exploring the immunomodulatory potential of traditional remedies in the treatment of various inflammatory diseases [8,9,25]. It has been demonstrated that double-stranded DNA can incorporate various TCM molecules, such as wogonin, resveratrol, curcumin, and baicalin [26–30]. This is primarily achieved through electrostatic adsorption, where small molecular TCMs remain stably adsorbed between the DNA double strands and enter cells along with tFNA after drug washout. In comparison to the individual use of free wogonin or tFNA, the utilization of tFNA-wogonin complexes has demonstrated a significant inhibitory ef-

fect on the expression of inflammatory mediators and matrix metalloproteinases. This effect was particularly notable in the context of promoting cartilage tissue regeneration within a rat osteoarthritis model. The observed mechanism underlying these positive outcomes appears to be associated with the enhanced water solubility and improved cell permeability facilitated by tFNA [25]. Similarly, the application of tFNA-resveratrol (RSV) complexes has exhibited noteworthy effects on the inflammatory state in mice subjected to a high-fat diet. This includes the inhibition of Th1 and Th17 cell activation, concurrent promotion of Th2 and Treg cell activation, and the reversal of M1 macrophage polarization toward the M2 phenotype [8,9]. These findings highlight the potential of tFNA-based delivery systems in modulating immune responses and addressing inflammatory conditions through diverse pathways. Furthermore, investigations into curcumin and its analogs, known to bind to DNA through thymine O2 and guanine N7, have revealed that tFNA-curcumin complexes exert a more pronounced down-regulation of inflammation-related cytokines compared to free curcumin [8]. This suggests that the incorporation of curcumin into tFNA structures enhances its anti-inflammatory effect, potentially through improved delivery and cellular uptake mechanisms.

Shifting focus to the challenges associated with the clinical application of small molecular weight drugs, like doxorubicin (DOX) and fluorouracil, several obstacles have been identified, including low cellular uptake, hydrophobic properties, lack of target specificity, and multi-drug resistance (MDR). The role of tFNA in overcoming these obstacles has been elucidated through various mechanisms. Notably, tFNA plays a crucial role in reversing MDR by amplifying intracellular drug accumulation, curbing drug efflux, and regulating the cell cycle. Both Kim and our research team have independently constructed self-assembled DNA tetrahedral nanoparticles designed to physically transporting DOX to resistant breast cancer cells, presenting a promising avenue for addressing multi-drug resistance in cancer treatment [31–33]. This innovative approach showcases the potential of tFNA as a versatile carrier for improving the effectiveness of chemotherapeutic agents in overcoming drug resistance and enhancing their therapeutic impact in clinical settings. In particular, tFNA can interact with small molecular weight drugs through their double helical structure, allowing efficient transport of these drugs into living cells.

Due to excessive antibiotic usage, which has led to the rise of multi-drug resistant superbug, there is an urgent need to create new antimicrobial agents, particularly innovative antibiotic delivery systems. Consequently, our endeavors have focused on creating a delivery system based on tFNA suitable for various types of microorganisms. Employing a low-temperature direct incubation method, we successfully engineered tFNA loaded with ampicillin. The tFNA-ampicillin complex, approximately 33.4 nm in size, has exhibited heightened uptake rates by methicillin-resistant *Staphylococcus aureus* (MRSA) bacteria. This was accompanied by characteristic membrane disintegration and morphological changes, thereby validating its efficacy against MRSA [34]. Broadening the scope of our research, we delved into loading erythromycin onto tFNA to augment its penetration through *Escherichia coli*'s cell membrane. This tactic sought to bolster bacterial uptake and mitigate drug resistance [35]. Additionally, we employed electrostatic interactions to encapsulate the antimicrobial peptide GL13K on tFNA. *In-vitro* experimental results demonstrated that GL13K-tFNA induced bacterial membrane instability in *E. coli*. Moreover, it shielded the GL13K peptide from degradation in a proteinase-rich extracellular environment, affirming the positive role of tFNA in antibacterial therapy (Fig. S5 in Supporting information) [36]. Extending our investigation to another antimicrobial peptide-like molecule, histatin 5, we observed more effective transport into *Candida albicans* with the assistance of tFNA. This modified histatin 5 exhibited superior stability in serum compared to its free form. Notably, tFNA-

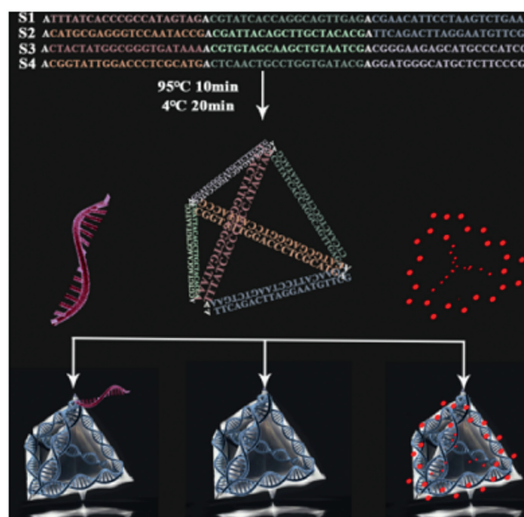


Fig. 1. The fabrication of tFNA includes the blending of single-stranded DNA, followed by rapid thermal annealing. tFNA can be further upgraded to carry oligonucleotides or small molecular drugs through various means. Ultimately, a pyramid-shaped three-dimensional tetrahedral structure is formed.

modified histatin 5 heightened the formation of intracellular reactive oxygen species, induced potassium efflux, and bolstered its antifungal potency against *Candida albicans* (Fig. 1) [37].

6. The biological features of tFNA

6.1. Enhanced endocytosis

Exogenous biomaterials like single-stranded or double-stranded DNA, which possess anionic characteristics, are essentially inert substances incapable of permeating cell membranes. A distinctive advantage offered by tFNA is its unique capability to undergo endocytosis by cell membranes, a feature seldom found in other DNA structures. This phenomenon can be attributed to the distribution of positive charges on the outer side and negative charges on the inner side of the membrane in its quiescent state. Consequently, owing to its negative charge, tFNA exhibits a natural attraction that facilitates its traversal across the membrane [38]. Additionally, the negative charge of the tFNA makes it prone to binding with proteins, reducing the probability of clearance [39]. The membrane affinity of tFNA is relatively beneficial in various biomedical applications [40]: (1) this configuration amplifies the attraction between tFNA and various membrane targets, including nuclear proteins, thereby fortifying their interaction [41]; (2) it allows a large quantity of tFNA to approach the membrane, thus promoting endocytosis [42]. Fundamentally, tFNA provides a molecular delivery tool with multifunctional potential [11]. Through total internal reflection fluorescence (TIRF) microscopy during co-cultivation with HeLa cells, the real-time tracking of Cy3-labeled tFNA revealed a two-stage endocytic process: first, a period of random movement for membrane-bound tFNA (>45 s), followed by a rapid internalization process (≈ 15 s). Vesicle-dependent pathways predominantly mediate this endocytotic process, ultimately directing tFNA to lysosomes within the cell. Beyond their impact on live cells, tFNA has also enhanced the efficacy of drug uptake by microorganisms. Microbes' resistance to DNA molecules and diverse drugs arises from their robust bacterial walls and the drug efflux mechanisms characteristic of multidrug resistance. While conventional transfection carriers, like cell-penetrating peptides, have gained considerable attention, their inherent cytotoxicity and immunogenicity pose significant challenges for clinical applications.

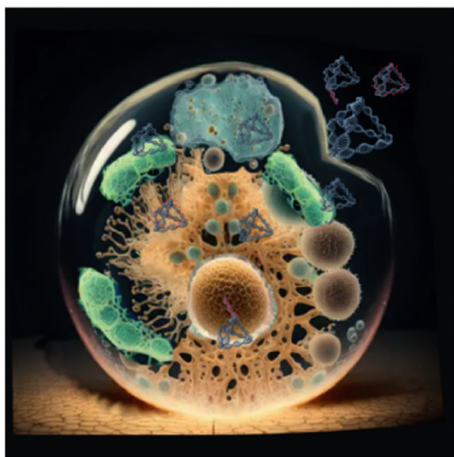


Fig. 2. tFNA-based systems enter cells through endocytosis, distribute in the cytoplasm and organelles to exert various biological functions and eventually end up in the lysosomes.

Thus, we have pioneered the development of the first antibacterial complex based on tFNA, termed asPNA-tFNA. Notably, compared to individual asPNA, tFNA significantly boosts the uptake efficiency of ftsZ-asPNA by MRSA cells, enabling targeted inhibition of the ftsZ gene to curb bacterial growth (Fig. 2) [43].

6.2. Reactive oxygen species (ROS) clearance

Uncontrolled oxidative stress stands as a pivotal contributor to the pathogenesis of diverse diseases. Mitochondrial dysfunction sparks an overproduction of ROS, directly assaulting cellular proteins and lipids, thereby instigating oxidative stress and subsequent inflammation [44]. This cascade is perpetuated by the activation of complement component 5a, intensifying inflammatory responses. This, in turn, triggers cascades in cytokine production, amplifying tissue damage and fostering organ dysfunction [45]. Our research has underscored the potential of tFNA in ROS scavenging, presenting a promising avenue in various disease models [46–49]. The capability to eliminate ROS is intrinsically linked to the DNA composition itself, and the structural intricacies of tFNA significantly augment its clearance efficiency compared to single-stranded counterparts. As elucidated in pertinent studies, tFNA demonstrates the capacity to permeate the cell membrane and undergo extensive endocytosis. This positions tFNA as a compelling contender in the competition for ROS oxidation processes, establishing its efficacy as a robust ROS scavenger across diverse disease contexts [46–49].

6.3. In vivo distribution

Tian *et al.* initially observed a swift presence of fluorescently labeled tFNA in the kidneys and subsequent migration to the bladder in a mouse model, indicating a notably efficient renal uptake and accumulation. These findings align with corroborating results from pertinent studies [50,51]. Recent investigations have unveiled additional pathways, revealing the rapid journey of tFNA to the liver and gallbladder post intravenous injection, followed by customary renal concentration and bladder accumulation [52–54]. The aggregation of nano-sized particles, ranging between 50 nm and 200 nm, within the liver sinusoids hints at potential liver accumulation of tFNA. Additionally, tFNA has exhibited an affinity for binding with serum protein, presenting a passive strategy for liver targeting [55]. Beyond intravenous administration, *in situ* injection emerges as a viable approach for tFNA. Utilizing a specialized catheter linked to the right lateral ventricle in mice for injecting tFNA-loaded siRNA,

this complex sustains presence in the cerebrospinal fluid for at least an hour without apparent adverse effects on other vital organs. Diversified chemical modifications offer researchers novel avenues for drug delivery. For instance, coupling tFNA with nuclear-targeting ligands like AS1411 manifests rapid accumulation in tumors [56]. Similar tumor-targeting effects are attainable by combining tFNA with tumor-penetrating peptides and other modified ligands [57]. Furthermore, the permeability of the blood-brain barrier can be altered by tFNA loaded with a 19-molecule peptide from the human Kunitz domain. In essence, the versatility of tFNA can be harnessed through diverse modifications, catering to the specific targeting needs of varied organs and biological systems.

6.4. Biostability

tFNA is endowed with three characteristics in drug transport: (1) biostability of under physiological or pathological conditions; (2) cell membrane permeability; (3) structural integrity and duration of distribution within cells [58]. A growing body of evidence indicates the remarkable resilience of DNA nanostructures against nuclease degradation. Specifically, these nanostructures exhibit a notable resistance for up to 42 h in the presence of fetal bovine serum (FBS) [59]. Furthermore, they maintain their structural integrity even after a 24-h incubation in 50% non-inactivated FBS, albeit experiencing partial degradation within 2 h under the same conditions [22]. Our recent investigations have corroborated these findings, revealing that more than 50% of tFNA functional systems endure a 12-h incubation in 10% FBS [60]. In the realm of cellular interactions, co-localization studies demonstrate the enduring presence of both fluorescence colors in live cells after an 8-h cultivation period, which underscores the robust biostability of dual-labeled Cy3 and Cy5 tFNA. Additionally, measurements of Förster resonance energy transfer (FRET) indicate that DNA tetrahedra maintain their integrity inside cells for at least 48 h [61]. Moving from *in-vitro* studies to *in-vivo* observations, our recent work utilizing an *in-vivo* imaging system revealed a rapid accumulation of Cy5-tFNA within the first 10 min after intravenous injection. Interestingly, these nanostructures were efficiently cleared from the kidneys within 60 min, showcasing their dynamic behavior *in vivo* [62]. Moreover, the circulation time of tFNA (with a half-life, $t_{1/2}$, of 24.2 min) surpasses that of siRNA (with a half-life, $t_{1/2}$, of 6 min). This discrepancy underscores the relative biological stability of tetrahedra and emphasizes the feasibility of utilizing tFNA as a carrier for different types of RNA and aptamers [24].

7. Biological applications of tFNA-based systems

7.1. Applications in the skin and soft tissue

tFNA has been proven to stimulate cell proliferation in skin cells by activating the Wnt/ β -catenin pathway following injury [63]. Employing real-time cell analysis (RTCA), it has been observed that the proliferation rate of fibroblasts reaches its peak after exposure to 250 nmol/L tFNA for 24 h (Fig. S1 in Supporting information). This heightened proliferative response is potentially linked to the upregulation of cyclin-dependent kinase-like 1 (CDKL1), indicating its role in regulating the cell cycle [64]. Delving into the epigenetic impact of tFNA on adipose-derived stem cells (ASCs) proliferation, it was discovered that the DNA hypermethylation of the Dlg3 gene promoter mediated the promotion by tFNA on ASC proliferation and the concurrent reduction in cell apoptosis [65]. Furthermore, in the presence of tFNA, the migration of rat adipose-derived stem cells underwent significant enhancement. This molecular modulation involved the downregulation of long non-coding RNA XLOC 010623, as well as the downregulation of Rac 1 and Tiam 1 culminating in the upregulation of Rho-associated coiled coil contain-

ing protein kinase 2 (ROCK2), Ras homolog gene family member A (RHOA) and vinculin [66]. To assess the potential of tFNA in promoting wound healing, an examination of its effects on cell behavior and vascularization was conducted. Following treatment with 250 nmol/L tFNA *in vitro*, there was an observed enhancement in the migration and proliferation of corneal epithelial cells, suggesting a promising role in wound healing [67]. The clinical assessment and histological examination of a rat corneal alkali burn model revealed a significant enhancement in corneal transparency and re-epithelialization of corneal wounds upon tFNA treatment. Regarding skin defect healing, a dosage of 125 nmol/L tFNA expedited skin wound closure, exhibiting a markedly increased rate of healing compared to the control group [68]. Analysis on the 14th and 21st days, utilizing hematoxylin and eosin staining for epithelial tissue, reduced scar areas and diminished inflammatory cell infiltration were observed in the group treated with tFNA. Moreover, tFNA treatment substantially mitigated skin fibrosis, evidenced by a notable reduction in the expression of inflammatory factors, including interleukin-1 β (IL-1 β) and tumor necrosis factor- α (TNF- α). In both epidermal formation cells (HaCaT cells) and fibroblasts, it was validated that tFNA-induced skin wound healing operated through the mediation of the protein kinase B (AKT) signaling pathway. Notably, tFNA has also exhibited positive effects on diabetic wound healing as well [69]. Treatment with tFNA in a diabetic human umbilical vein endothelial cells (HUVECs) model resulted in heightened cell migration, proliferation and vascularization, coupled with an increased formation of vessel-like structures in Matrigel scaffolds. In diabetic rats, the administration of 250 nmol/L tFNA on a daily basis expedited wound healing, yielding a healed area of 81.72% on day 4 and 98.55% on day 10, in stark contrast to 59.47% and 82.46% in control group, respectively. Observations from Masson staining and CD34 immunohistochemistry indicated an augmentation in blood vessels and wall cells, alongside increased collagen and tissue fiber deposition in the diabetic group. Furthermore, the utilization of tFNA loaded with fibrosis-promoting molecules demonstrated an inhibitory effect on epithelial-mesenchymal transition, decreased inflammation, and reduced skin collagen content. These findings have signified the potential of tFNA in the treatment of conditions related to upper eyelid ptosis [70]. Employing tFNA loaded with VEGF has shown enhanced efficacy in accelerating endothelial cell proliferation and migration, promoting tube formation, sphere budding, and facilitating blood vessel development, both *in vitro* and *in vivo* [71]. In a skin aging model, the use of tFNA loaded with a miR-31 inhibitor demonstrated noteworthy anti-aging effects. This was accompanied by observations of enhanced skin penetration capability and RNA delivery efficiency, indicating the versatility, stability, and delivery proficiency of tFNA [72]. For wound healing therapy, local injection of tFNA at concentrations ranging between 125 nmol/L and 250 nmol/L proved to be a satisfactory method, notably lower than the commonly employed concentration of tFNA for intravenous injection.

7.2. Applications in the bone-cartilage-muscle system

The absence of blood vessels, nerves, and lymph in joint cartilage poses a formidable challenge for tissue regeneration. In response to this obstacle, we employed tFNA to treat primary chondrocytes, leading to the observation of remarkable cartilage regeneration. Within our study, the utilization of a 250 nmol/L concentration of tFNA effectively preserved the cell phenotype of rat primary chondrocytes. This restoration manifested as a shift from a fibroblast-like morphology to a normal rounded and three-dimensional shape, a phenomenon attributed to the activation of the Notch signaling pathway [73]. Additionally, concentration-dependent impacts on chondrocyte proliferation and migration

rates were evident post-tFNA treatment within the range of 62.5–250 nmol/L [73,74]. Moreover, tFNA has exhibited a significant augmentation in the number of autophagosomes in chondrocytes. Following treatment with 250 nmol/L tFNA, the mRNA expression of phosphoinositide 3-kinase (PI3K) and AKT increased, while the expression of mammalian target of rapamycin (mTOR) at transcriptional level was reduced. This observation implies that tFNA could regulate chondrocyte autophagy by the PI3K/AKT/mTOR pathway [62]. In experiments aiming to boost chondrocyte proliferation with tFNA, their inclusion in chondrogenic induction culture medium heightened the chondrogenic capability of mesenchymal stem cells (MSC) by increasing the phosphorylation of Smad2/3 (Fig. S3 in Supporting information). Notably, in animal models, tFNA injection improved the therapeutic outcomes for cartilage defects compared to other treatments without tFNA [75]. Further experiments have targeted bone differentiation using tFNA loaded with miR-26a. This resulted in a notable increase in the expression of proteins and genes linked to the Wnt/ β -catenin signaling pathway. The osteogenic differentiation capability of bone marrow mesenchymal stem cells (BMSCs) was boosted, evident in the augmented expression of ALP and the formation of calcium nodules in MSCs. This has convincingly illustrated that tFNA could induce MSC osteogenic differentiation by activating the Wnt signaling pathway [76]. Moreover, within an *in-vitro* model of osteoarthritis, tFNA was laden with flavonoid-calcium to form the wogonin/tFNA complex. This intricate formation proved effective in assuaging inflammation by orchestrating a down-regulation of inflammatory mediators and matrix metalloproteinases. Notably, when administered to rats afflicted with osteoarthritis, the application of tFNA resulted in a noteworthy elevation in both type II collagen and proteoglycan levels, acting as a safeguard against cartilage degradation [25]. In a recent investigation centered around rheumatoid arthritis (RA), a strategic integration of miR-23b into the tFNA structure enhanced the stability of miR-23b, facilitating its effective delivery and release *in vivo*. The treatment involving tFNA-miR23b emerged as a potent alleviator of synovial inflammation, manifesting through the inhibition of inflammatory cell infiltration and suppression of synovial hyperplasia. Furthermore, this treatment demonstrated a pronounced hindrance to the degradation of the cartilage matrix and the generation of osteoclasts, thereby fortifying the protection of the joint structure [60]. In treating ankylosing spondylitis (AS), tFNA managed to inhibit local and systemic inflammation as well as ectopic ossification in the intervertebral disc tissue to halt disease progression. In the corresponding *in-vitro* experiments, tFNA regulated the biological behavior of AS primary chondrocytes through the IL-17 pathway to inhibit the secretion of various pro-inflammatory cytokines. Osteogenesis in chondrocytes was also inhibited at the transcriptional level, achieving the ultimate goal of alleviating AS-related symptoms and improve patients' quality of life (Fig. S4 in Supporting information) [77]. In a parallel investigation, the utilization of tFNA for loading puerarin (Pue) not only succeeded in enhancing the stability, biocompatibility, and tissue utilization of Pue but also marked a transformative leap in therapeutic efficacy. This innovative strategy has proved its effectiveness by restoring bone function and alleviating apoptosis induced by high-dose glucocorticoids in BMSCs. These effects were orchestrated through the modulation of the hedgehog and AKT/Bcl-2 pathways, ultimately preventing femoral head necrosis in a meticulously conducted experimental study involving rats [78]. Equally noteworthy is the revelation that tFNA could exert a profound influence on bone fractures associated with osteoporosis, propelling osteogenesis and vascular regeneration. The potential mechanism behind this phenomenon was speculated to involve the regulation of the FoxO1-related SIRT1 pathway, showing the multifaceted impact of tFNA in orchestrating regenerative processes within bone tissue [79]. Expanding the

scope of their impact, tFNA ventured into the realm of muscle metabolism, yielding substantial enhancements in both function and endurance in an elderly mouse model. The microscopic landscape of muscle fibers underwent favorable morphological changes, which presented a visual testament to the positive outcomes of tFNA intervention. Notably, in the face of dexamethasone-induced muscle atrophy *in vitro*, tFNA treatment emerged as a potent intervention to inhibit mitochondria-mediated apoptosis and pave the way for structural and functional improvements [80]. This not only confirms the versatility of tFNA but also points towards their potential as a transformative force across diverse physiological domains.

7.3. Applications in the nervous system

In light of the inherent limitations in the regenerative and self-healing capacities of nerve cells, the transplanting of neural stem cells (NSCs) has emerged as a pivotal therapeutic strategy for neural repair. Recognizing the paramount importance of methods that can effectively stimulate the proliferation and differentiation of NSCs, there has been a burgeoning interest in the exploration of innovative avenues. Notably, one such transformative approach involves the utilization of tFNA. Studies have elucidated that tFNA exhibited a remarkable capacity to foster the migration and proliferation of neural ectoderm stem cells *in vitro*. Furthermore, it demonstrated the ability to induce neuronal differentiation by intricately modulating the Notch pathway (Fig. S2 in Supporting information) [81,82]. Expanding beyond the confines of the petri dish, the application of tFNA in conjunction with neural stem cells has yielded promising outcomes in a rat spinal cord injury (SCI) model [83]. At the culmination of the 8-week study period, rats treated with tFNA-NSC showcased a significantly elevated Basso-Beattie-Bresnahan score in comparison to counterparts treated with tFNA and NSC alone. This marked improvement underscored enhanced motor and sensory recovery facilitated by the synergistic action of tFNA and neural stem cells. Complementary evidence was derived from heightened Nestin immunofluorescence in the tFNA-NSC treated group, providing insight into the impact of tFNA on NSC survival and proliferation. Turning the focus towards neurodegenerative conditions, the accumulation of amyloid- β ($A\beta$) in the brain stands as a recognized hallmark in the pathogenesis of Alzheimer's disease. Specifically, tFNA has exhibited a remarkable ability to thwart $A\beta$ -induced cytotoxicity in PC12 cells to rescue these cells from excessive death [84]. In a quantitative shift from cellular studies to *in vivo* models, rats pre-treated with tFNA displayed a significantly reduced mortality rate in $A\beta$ -treated PC12 cells. This protective effect was further validated in the behavioral assessments, where rats exhibited a substantially lower escape latency in the Morris water maze test on the 5th day. This outcome was indicative of improved memory and learning abilities in the context of AD, establishing the *in-vivo* protective capacity of tFNA in an Alzheimer's disease rat model [85]. In summary, the application of tFNA represents a transformative paradigm in the field of neural repair and neuroprotection. From augmenting NSC function in spinal cord injuries to mitigating the cytotoxic effect of $A\beta$ in Alzheimer's disease, the multifaceted potential of tFNA holds promise for advancing therapeutic strategies in neurobiology and regenerative medicine. The potential mechanism has involved a reduction in aberrant Nissl-stained cell count within the hippocampus post intravenous tFNA injection. Furthermore, tFNA has demonstrated their utility in cell models of Parkinson's disease, manifesting an inhibitory effect on the apoptosis in PC12 cells treated with 1-methyl-4-phenyl-1,2,3,6-tetrahydropyridine (MPTP) through the AKT/PI3K signaling pathway [86]. Altogether, tFNA has emerged as a promising neurorestorative and neuroprotective biomaterial for both Parkinson's and Alzheimer's diseases. In

a study on facial nerve injury, tFNA was found to modulate the NGF/PI3K/AKT nerve repair pathway, fostering cell proliferation and migration for nerve repair in the injured area [87]. Specifically, tFNA increased the expression of markers associated with axonal growth and myelination, expediting the recovery of tissue structure and facilitating the restoration of nerve conduction and muscular function. In a study involving stroke-related astrocytes, tFNA was observed to impede calcium overload and ROS generation triggered by oxygen-glucose deprivation/reoxygenation (OGD/R), thereby shielding astrocytes from apoptosis. Simultaneously, tFNA downregulated the Toll-like receptors (TLRs)/nuclear factor kappa-B (NF- κ B) signaling pathway, presenting a possible mechanism for astrocyte protection in stroke [88]. Leveraging tFNA for miRNA-22 delivery amplified communication between macrophages and Schwann cells (SCs), leading to a more proficient recovery of peripheral nerve function. It was revealed that tFNA carrying miRNA-22 expedited macrophage recruitment, inducing a heal-promoting M2 phenotype to reestablish the microenvironment after injury. Moreover, tFNA loaded with miRNA-22 rapidly initiate adaptive intracellular reprogramming in SCs, further promoting axon regeneration and remyelination [89]. In an epilepsy study, tFNA was capable of penetrating the blood-brain barrier (BBB) and effectively suppressed the activation of M1 microglial cells and the proliferation of A1 reactive astrocytes in the mouse hippocampus following prolonged seizures. Additionally, tFNA demonstrated an inhibitory effect to downregulate the level of glutamine synthetase and alleviate oxidative stress in astrocytes, leading to a decrease in glutamate production and thus mitigating glutamate-mediated neuronal excitotoxicity. Furthermore, tFNA promoted the internalization of α -amino-3-hydroxy-5-methyl-4-isoxazolepropionic acid receptors (AMPA) in the postsynaptic membrane by regulating AMPAR endocytosis. This regulatory mechanism might account for the decrease in calcium influx to lower the frequency of hyperexcitability and spontaneous epileptic seizures ultimately [90]. In conclusion, tFNA exhibits a remarkable capacity to promote neuroprotection and neural regeneration *in vitro*, thus effectively alleviating damage in experimental nerve injury animal models. Importantly, tFNA has also enhanced the proliferation of neural stem cells. When combined with neural stem cell treatment, tFNA could achieve the most favorable outcomes in terms of transplanted cell survival, motor function recovery in rats, and tissue regeneration at the spinal cord injury site, with minimal formation of glial scar tissue [91].

7.4. Application in the immune system

tFNA has exhibited the capability to modulate the transcription level of inducible nitric oxide synthase (iNOS), thereby diminishing nitric oxide (NO) production after lipopolysaccharide (LPS) induction in RAW264.7 macrophage cells. Concerning the polarization of macrophages into M1/M2 phenotypes, tFNA can stimulate the expression of iNOS, which is an indicative marker of the M1-type macrophages, while concurrently suppressing the expression of the M2 marker arginase. Notably, when compared to the LPS-treated group, the tFNA-treated group manifested a notable decline in the level of several important inflammatory cytokines including IL-1 β , IL-6, and TNF- α , signaling a mitigated inflammatory response [46]. In a separate investigation, it was observed that tFNA loaded with osteogenic peptide (OGP) provided protection to bone marrow stromal cells against DNA damage and apoptosis induced by 5-fluorouracil (5-FU). OGP-tFNA activated extracellular signal-regulated kinase (ERK) signaling while downregulating the expression of apoptosis-related proteins. Furthermore, OGP-tFNA alleviated the inhibition of chemotherapy-induced expression of hematopoietic-related cytokines, thereby shielding hematopoietic cells and their micro-environment from

severe damage induced by chemotherapy. This dual action as well contributed to the promotion of hematopoietic regeneration [92]. Additionally, our investigations revealed that tFNA, when loaded with miR-155, could induce macrophages to polarize towards the anti-angiogenic M1 type. Upon injection into the vitreous of laser-induced choroidal neovascularization (CNV) mice, miR-155-loaded tFNA significantly reduced the area of CNV and effectively inhibited vascular leakage in the context of laser-induced choroidal neovascularization [93]. This demonstrates that tFNA loaded with miR-155 could ameliorate the inflammatory responses of CNV by regulating macrophage polarization [93]. Another study has demonstrated that *in vivo*, tFNA loaded with miR-155 could resist oxidative stress by promoting T-cell proliferation, thereby alleviating splenic and thymic damage as well as hematopoietic suppression in cyclophosphamide-induced immunosuppressive mice. *In vitro*, tFNA loaded with miR-155 induced the differentiation of immature dendritic cells (DC) into mature DC *via* regulating the ERK1/2 pathway and transform M0 macrophages into M1 type through the NF- κ B pathway to enhance the surveillance capabilities of antigen-presenting cells [94]. The breakdown of immune tolerance triggers the destruction of insulin-producing β cells by autoimmune responses, culminating in type 1 diabetes. In a pertinent investigation, tFNA has been utilized to suppress autoreactive T cells and prompt the induction of regulatory T cells (Tregs) in order to restore immune tolerance. This treatment with tFNA has demonstrated its capability to sustain normal blood glucose levels and reduce the incidence of diabetes. Moreover, it has shown certain efficacy in preserving the quality and functionality of β cells, augmenting Treg populations, and curbing autoreactive T cells, thus facilitating the restoration of immune tolerance [95]. Furthermore, the incorporation of RSV into tFNA has been identified as beneficial for ameliorating insulin resistance by mitigating the inflammatory milieu. In the realm of adaptive immunity, this formulation has exhibited the ability to impede the activation of Th17 and Th1 cells while fostering the generation of Tregs and Th2 cells to influence the distribution of T cell subtypes [32]. Advanced glycation end-products (AGEs) are crucial in instigating multi-organ dysfunction. The interplay between AGEs and their primary receptor (RAGE) initiates the propagation of intracellular inflammatory and apoptotic signals, ultimately contributing to various diabetic complications. Employing tFNA loaded with siRNA targeting RAGE for diabetes management has shown persistent down-regulation of RAGE expression, thereby exerting an antioxidant effect and alleviating inflammation *via* the NF- κ B pathway [96]. Additionally, another investigation highlights that tFNA could impede c-Jun N-terminal kinase (JNK) and ERK phosphorylation *via* the JNK signaling pathway to significantly curb the secretion of interferon γ (IFN γ), an activator of T cells, meanwhile imposing no effect on TNF secretion. Comparable immunomodulatory effects of tFNA have also been observed in autoreactive T cells of individuals with neuromyelitis optica spectrum disorder (NMOSD) [97]. Sjögren's syndrome (SS) stands out as one of the prevalent autoimmune disorders, marked by an overactive infiltration of lymphocytes into exocrine glands, leading to symptoms such as dry mouth and dry eyes. Recent findings indicated the efficacy of tFNA treatment in curbing inflammation and promoting saliva secretion in mice. This intervention proved instrumental in reinstating the synthesis of specific functional proteins and preserving the structural integrity of submandibular gland acinar cells. In the course of the *in-vivo* experiments, tFNA treatment not only steered a higher proportion of T cells towards Tregs but also hampered T helper cell responses. Parallel outcomes were evident in responses of B cells, manifesting a reduction in the number of germinal center B cells and plasma cells, coupled with a notable upswing in the number of regulatory B cells. The initiation mechanism for Tregs appeared to be linked to alterations in serum cytokine levels. Modifications in T cell

subsets, particularly adjustment in Th cells, were also likely to impact the differentiation of B cells correspondingly [98].

7.5. Applications in the genitourinary and digestive systems

In a study addressing bladder outlet obstruction, tFNA treatment has demonstrated the potential to ameliorate bladder fibrosis and functional impairment induced by the obstruction. This was achieved by hindering M2 macrophage polarization and the macrophage-myofibroblast transition (MMT) process. Specifically, tFNA stimulated macrophage polarization towards the anti-inflammatory M2-type and regulate MMT process by deactivating signal transducers and activators of transcription (Stat) and the transforming growth factor- β 1 (TGF- β 1)/Smad pathway independently [99].

Acute kidney injury, identified as an independent risk factor and promoter of chronic kidney disease progression, has also witnessed promising results with typhaneoside-loaded tFNA. This treatment showcased precise targeting capability of tFNA for mitochondria and renal tubules. It exerts both anti-apoptotic and antioxidant effects, thereby fostering the recovery of mitochondrial and renal function [100]. Liver failure, marked by hepatocyte necrosis, poses a significant health challenge. Notably, tFNA has been reported to activate the Wnt and Notch signaling pathways, stimulating *in-vitro* hepatocytic proliferation by modulating the cell cycle and the P53 signaling pathway. Furthermore, tFNA treatment exhibited positive effects on hepatocytic proliferation and hepatic tissue regeneration in mice subjected to drug-induced liver injury. This multifaceted impact prevented the occurrence of acute liver failure and therefore reduced associated mortality [101]. Using tFNA loaded with siCCR2 has also reduced liver fibrosis. Compared to pure siCCR2 molecules, the tFNA-siCCR2 complex prolonged liver retention time after intraperitoneal injection and mainly co-localized in macrophages and endothelial cells. Single-cell RNA sequencing and experimental validation suggested that tFNA-siCCR2 restored the immune cell landscape and constructed an anti-fibrotic niche by inhibiting the aggregation of neutrophils and pro-fibrotic macrophages in the mouse fibrotic liver. From a molecular perspective, the tFNA-siCCR2 complex decreased the level of inflammatory factors by deactivating the NF- κ B signaling pathway [102]. Severe acute pancreatitis (SAP) is regarded as an inflammatory disease of the pancreas characterized by tissue damage and cell necrosis. Beyond its localized impact on the pancreas, SAP sets off systemic inflammation, culminating in multi-organ failure and potential fatality. Administering tFNA to mice with SAP has emerged as a potent intervention, effectively curbing inflammation and thwarting pathological cell death. Post-tFNA treatment, notable shifts manifested in the serum levels of pancreatic inflammation-related biomarkers. This tFNA treatment included a discernible reduction in the expression level of specific inflammatory cytokines implicated both locally and systemically, accompanied by modifications in the expression level of proteins associated with cell death and apoptosis [7].

7.6. Applications in antitumor therapy

For numerous decades, temozolomide (TMZ) has stood as a cornerstone in the therapeutic arsenal against glioblastoma multiforme (GBM). However, the swift emergence of drug resistance and the consequential bone marrow suppression present formidable challenges to the efficacy of GBM treatment. The incorporation of TMZ onto tumor-targeted functional nucleic acid nanocarrier has amplified its cytotoxic impact on four distinct GBM cell lines by instigating cell apoptosis and autophagy pathways. Notably, this approach exhibited enhanced effectiveness in eradicating TMZ-sensitive cells when juxtaposed with the sole application of TMZ.

Moreover, tFNA-TMZ was proved adept at mitigating the resistance observed in TMZ-resistant cells by modulating the expression of O6-methylguanine-DNA-methyltransferase. To enhance the blood-brain barrier penetration, tFNA underwent structural modification with GS24, which is a DNA aptamer that can bind to transferrin receptors in mouse brain endothelial cells selectively [103]. In an alternative approach within the realm of glioblastoma treatment, another study has utilized tFNA to load GMT8 and Gint4.T—two ligands with specific affinity for U87MG cells. This amalgamation resulted in a complex denoted as Gint4.T-tFNAs-GMT8 (GTG), which demonstrated efficient internalization by both U87MG and bEnd.3 cells and successfully traversed the blood-brain barrier *in vivo*. To further elevating its therapeutic potential, paclitaxel was loaded onto GTG, augmenting its efficacy against glioblastoma. This comprehensive strategy curtailed U87MG cell proliferation, migration, and invasion while concurrently inducing apoptosis [53]. Shifting the focus to malignant melanomas, a malignancy predominantly associated with Braf gene mutations, a distinct application of tFNA has emerged. Leveraging tFNA for the delivery of siBraf, coupled with the direct incorporation of AS1411 (a DNA aptamer) into tFNA, has enhanced the cellular uptake efficiency of siBraf. Results underscored the potency of tFNAs-AS1411-siBraf in suppressing Braf mRNA expression compared to its free counterpart [104]. To suppress the SLC31A1 gene, which is responsible for encoding the primary transmembrane copper transporter (CTR1), has been proven to be a potent strategy to diminish the aggressiveness of pancreatic cancer by lowering intracellular copper concentrations. Employing tFNA for the delivery of siCTR1 or miR-124 into PANC-1 cells robustly hampered CTR1 expression, resulting in a substantial blockade of copper uptake in comparison to conventional free RNA therapy. This targeted intervention has effectively hindered the advancement of pancreatic cancer, marking a significant stride in impeding its progression [105].

7.7. Applications in degenerative and infectious diseases

Elevated intracellular ROS production stands as a hallmark of oxidative stress, precipitating cellular dysfunction through processes like DNA fragmentation, protein modification, and lipid peroxidation. In the realm of combating aging and inflammatory diseases, tFNA has demonstrated notable antioxidant capabilities [106]. In an early investigation, our research successfully uncovered some compelling insights: RAW264.7 cells treated with tFNA exhibited a discernible reduction in ROS production when compared with the control group. In the absence of LPS, normal cells, regardless of tFNA treatment, displayed no significant variance in ROS production. The underlying mechanism of the antioxidant capacity of tFNA might involve the upregulation of the HO-1 gene, which is regarded as significant anti-oxidant and anti-inflammatory guardian, to accelerate biliverdin degradation or ferritin co-induction [107]. Motivated by these findings, a series of studies were undertaken to elucidate how tFNA exerted its anti-inflammatory and anti-degenerative effect by curtailing ROS release. This encompassed diverse conditions such as insulin resistance in type 1 diabetes, retinal ischemia-reperfusion injury [47], myocardial ischemia-reperfusion injury [108], acute kidney injury [109], bisphosphonate-related jawbone necrosis in macrophage polarization [48], and periodontitis [110]. Furthermore, degenerative diseases affecting the optic nerve, such as diabetic retinopathy and retinal artery occlusion, are also associated with ROS overproduction in retinal ganglion cells (RGCs) [111]. We then applied tFNA to treat RGCs induced by *tert*-butyl hydroperoxide (TBHP). Consistently, tFNA demonstrated a capacity to diminish the intracellular accumulation of excessive ROS, concurrently restoring nuclear morphology. The above findings have indicated that tFNA confers certain protective effect against oxidative stress by acti-

vating the AKT/Nrf2 signaling pathway and modulating oxidation-related enzymes. Oxidative stress is widely recognized for its potential to trigger cell apoptosis, disrupt metabolic equilibrium, and incite degenerative processes. Consequently, tFNA holds promise as a prospective therapeutic option for addressing both degenerative and inflammatory ailments. Sepsis, stemming from the infiltration of pathogenic microorganisms, prompts the heightened expression of TLRs, consequently fostering an unbridled escalation of inflammatory responses within cells. TLR2, a pivotal member of the TLR family, assumes a critical role in identifying innate immune reactions. Hence, impeding the expression and activation of TLR2 can stymie the synthesis and release of inflammatory agents, thus thwarting the onset of excessive inflammatory cascades. The utilization of tFNA laden with siTLR2 in anti-inflammatory interventions exhibited a discernible capacity to specifically curtail the LPS-triggered upsurge in TLR2 and diminish the release of inflammatory mediators in experimental sepsis induced by LPS [112].

8. Conclusion and prospects

tFNA exhibits substantial intracellular capabilities. Our investigations have revealed that various cell types and microorganisms display a notable proficiency in internalizing tFNA, surpassing the efficiency seen with single-stranded DNA. While the concentration of tFNA significantly influences cellular uptake rates, this impact comes at the expense of compromising cell toxicity. Consequently, for studies conducted at the cellular level, it is advisable to maintain concentrations below 250×10^{-9} mol/L. In animal models, considerations such as drug delivery pathways and enzyme degradation at target sites often necessitate the utilization of higher concentrations of tFNA, typically in the vicinity of 1000×10^{-9} mol/L.

Methods for functionalizing tFNA encompass direct connection or bridging facilitated by oligonucleotide complementary sequences, insertion into the DNA double helical structure, electrostatic interaction with drugs of small molecular weights, and even aggregation through polyethylene glycol (PEG) cross-linking to form larger particles. The choice of manufacturing method for functionalized tFNA nanostructure should be tailored to the intended application. For optimal gene silencing, it is advisable to employ no less than three ligands with proper spatial orientation to ensure successful fabrication. Consequently, to determine the number of target molecules and functional groups for gene silencing becomes a crucial consideration. Furthermore, the stability of the structure during assembly and in complex application environments is significantly influenced by the shape, size, secondary and spatial structure of the loaded nucleic acids or functional small molecule drugs. Likewise, careful consideration should be given to pre-assembled tFNA for drug delivery or pre-coupled molecules to single DNA strands for subsequent synthesis steps in the quick self-assembly of tFNA functional systems.

In conclusion, the biomedical applications of tFNA are underpinned by two primary foundations. The first revolves around the unique physical-chemical properties imparted by DNA, empowering tFNA with capabilities for genetic editing, regulation of cellular behavior, and clearance of ROS. The second foundation lies in the tetrahedral structure of tFNA, which enhances its internalization within biological systems and endows it with favorable editability. Leveraging these dual foundations, we are continuing to broaden the scope of biomedical applications for tFNA and its functional systems.

Declaration of competing interest

The authors declare that they have no known competing financial interests or personal relationships that could have appeared to influence the work reported in this paper.

Acknowledgments

This study was supported by National Key R&D Program of China (No. 2019YFA0110600), National Natural Science Foundation of China (Nos. 82370929, 81970916), Sichuan Science and Technology Program (No. 2022NSFSC0002), Sichuan Province Youth Science and Technology Innovation Team (No. 2022JDTD0021), Research and Develop Program, West China Hospital of Stomatology Sichuan University (No. RD03202302), Science and technology support plan project of Guizhou Provincial Department of science and technology (No. Qiankehe support[2022]General264).

Supplementary materials

Supplementary material associated with this article can be found, in the online version, at doi:10.1016/j.ccl.2024.109591.

References

- [1] N.C. Seeman, *Nature* 421 (2003) 427–431.
- [2] E. Winfree, F. Liu, L.A. Wenzler, N.C. Seeman, *Nature* 394 (1998) 539–544.
- [3] X.H. Guo, E.J. Huff, D.C. Schwartz, *Nature* 359 (1992) 783–784.
- [4] E. Tooker, *Science* 185 (1974) 1001.
- [5] D.Y. Zhang, G. Seelig, *Nat. Chem.* 3 (2011) 103–113.
- [6] W. Ma, Y. Zhan, Y. Zhang, et al., *Signal Transduct. Target. Ther.* 6 (2021) 351.
- [7] Y. Wang, Y. Li, S. Gao, et al., *Nano Lett.* 22 (2022) 1759–1768.
- [8] M. Zhang, X. Zhang, T. Tian, et al., *Bioact. Mater.* 8 (2022) 368–380.
- [9] Y. Li, S. Gao, S. Shi, et al., *Nano-Micro Lett.* 13 (2021) 86.
- [10] T. Tian, T. Zhang, S. Shi, et al., *Nat. Protoc.* 18 (2023) 1028–1055.
- [11] T. Zhang, T. Tian, R. Zhou, et al., *Nat. Protoc.* 15 (2020) 2728–2757.
- [12] W. Cui, X. Yang, X. Chen, et al., *Adv. Funct. Mater.* 31 (2021) 2105152.
- [13] Y. Yang, J. Zhu, W. Ma, et al., *Appl. Mater. Today* 24 (2021) 101098.
- [14] S.M. Douglas, A.H. Marblestone, S. Teerapittayanon, et al., *Nucleic Acids Res.* 37 (2009) 5001–5006.
- [15] J.N. Zadeh, C.D. Steenberg, J.S. Bois, et al., *J. Comput. Chem.* 32 (2011) 170–173.
- [16] J.P.K. Doye, H. Fowler, D. Prešern, et al., *Methods Mol. Biol.* 2639 (2023) 93–112.
- [17] D.N. Kim, F. Kilchherr, H. Dietz, M. Bathe, *Nucleic Acids Res.* 40 (2012) 2862–2868.
- [18] C.E. Castro, F. Kilchherr, D.N. Kim, et al., *Nat. Methods* 8 (2011) 221–229.
- [19] P.W.K. Rothemund, *Nature* 440 (2006) 297–302.
- [20] F. Zhang, S. Jiang, S. Wu, et al., *Nat. Nanotechnol.* 10 (2015) 779–784.
- [21] Z. Zhou, P. Zhang, L. Yue, I. Willner, *Nano Lett.* 19 (2019) 7540–7547.
- [22] J. Li, H. Pei, B. Zhu, et al., *ACS Nano* 5 (2011) 8783–8789.
- [23] Q. Li, D. Zhao, X. Shao, et al., *ACS Appl. Mater. Interfaces* 9 (2017) 36695–36701.
- [24] H. Lee, A.K.R. Lytton-Jean, Y. Chen, et al., *Nat. Nanotechnol.* 7 (2012) 389–393.
- [25] S. Siron, C. Yang, T. Taoran, et al., *Bone Res.* 8 (2020) 6.
- [26] N.M. Khan, I. Ahmad, M.Y. Ansari, T.M. Haqqi, *Chem. Biol. Interact.* 274 (2017) 13–23.
- [27] Y. Sun, S. Bi, D. Song, et al., *Sens. Actuators B: Chem.* 129 (2008) 799–810.
- [28] G. Rusak, I. Piantanida, L. Mašić, et al., *Chem. Biol. Interact.* 188 (2010) 181–189.
- [29] S.C. Shen, W.R. Lee, H.Y. Lin, et al., *Eur. J. Pharmacol.* 446 (2002) 187–194.
- [30] M.S. Nair, A. Shukla, J. Biomol. Struct. Dyn. 38 (2020) 3087–3097.
- [31] K.R. Kim, H.Y. Kim, Y.D. Lee, et al., *J. Control. Release* 243 (2016) 121–131.
- [32] K.R. Kim, D-R. Kim, T. Lee, et al., *Chem. Commun.* 49 (2013) 2010.
- [33] X. Xie, X. Shao, W. Ma, et al., *Nanoscale* 10 (2018) 5457–5465.
- [34] Y. Sun, S. Li, Y. Zhang, et al., *ACS Appl. Mater. Interfaces* 12 (2020) 36957–36966.
- [35] Y. Sun, Y. Liu, B. Zhang, et al., *Bioact. Mater.* 6 (2021) 2281–2290.
- [36] Y. Liu, Y. Sun, S. Li, et al., *Nano Lett.* 20 (2020) 3602–3610.
- [37] R. Chen, D. Wen, W. Fu, et al., *Cell Prolif.* 55 (2022) e13206.
- [38] E. Akbari, M.Y. Mollica, C.R. Lucas, et al., *Adv. Mater.* 29 (2017) 1703632.
- [39] Y. Ahmadi, E. De Llano, I. Barišić, *Nanoscale* 10 (2018) 7494–7504.
- [40] H. Ding, J. Li, N. Chen, et al., *ACS Cent. Sci.* 4 (2018) 1344–1351.
- [41] X. Chen, F. Tian, M. Li, et al., *Global Challenges* 4 (2020) 1900075.
- [42] W. Ma, Y. Zhan, Y. Zhang, et al., *Nano Lett.* 19 (2019) 4505–4517.
- [43] Y. Zhang, W. Ma, Y. Zhu, et al., *Nano Lett.* 18 (2018) 5652–5659.
- [44] O. Boutaud, K.P. Moore, B.J. Reeder, et al., *Proc. Natl. Acad. Sci. U. S. A.* 107 (2010) 2699–2704.
- [45] T.V. Arumugam, I.A. Shiels, A.J. Strachan, et al., *Kidney Int.* 63 (2003) 134–142.
- [46] Q. Zhang, S. Lin, S. Shi, et al., *ACS Appl. Mater. Interfaces* 10 (2018) 3421–3430.
- [47] X. Qin, N. Li, M. Zhang, et al., *Nanoscale* 11 (2019) 20667–20675.
- [48] D. Zhao, W. Cui, M. Liu, et al., *ACS Appl. Mater. Interfaces* 12 (2020) 44508–44522.
- [49] S. Shi, T. Tian, Y. Li, et al., *ACS Appl. Mater. Interfaces* 12 (2020) 56782–56791.
- [50] T. Tian, T. Zhang, T. Zhou, et al., *Nanoscale* 9 (2017) 18402–18412.
- [51] D. Jiang, Z. Ge, H.J. Im, et al., *Nat. Biomed. Eng.* 2 (2018) 865–877.
- [52] Y. Tian, Y. Huang, P. Gao, T. Chen, *Chem. Commun.* 54 (2018) 9394–9397.
- [53] D. Xiao, Y. Li, T. Tian, et al., *ACS Appl. Mater. Interfaces* 13 (2021) 6109–6118.
- [54] G. Zhang, Z. Zhang, J. Yang, *Nanoscale Res. Lett.* 12 (2017) 495.
- [55] X. Liu, L. Wu, L. Wang, W. Jiang, *Talanta* 179 (2018) 356–363.
- [56] Z. Xia, P. Wang, X. Liu, et al., *Biochemistry* 55 (2016) 1326–1331.
- [57] Y. Zhang, S. Jiang, D. Zhang, et al., *Chem. Commun.* 53 (2017) 573–576.
- [58] R.A. Petros, J.M. DeSimone, *Nat. Rev. Drug Discov.* 9 (2010) 615–627.
- [59] J.W. Keum, H. Bermudez, *Chem. Commun.* (2009) 7036.
- [60] L. Wang, Y. Wang, T. Lu, et al., *Adv. Funct. Mater.* 23 (2023) 10749.
- [61] A.S. Walsh, H. Yin, C.M. Erben, M.J.A. Wood, A.J. Turberfield, *ACS Nano* 5 (2011) 5427–5432.
- [62] S. Shi, S. Lin, Y. Li, et al., *Chem. Commun.* 54 (2018) 1327–1330.
- [63] Q. Peng, X.R. Shao, J. Xie, et al., *ACS Appl. Mater. Interfaces* 8 (2016) 12733–12739.
- [64] K. Xia, H. Kong, Y. Cui, et al., *ACS Appl. Mater. Interfaces* 10 (2018) 15442–15448.
- [65] S. Lin, Q. Zhang, T. Zhang, et al., *ACS Appl. Mater. Interfaces* 10 (2018) 32017–32025.
- [66] S. Shi, Q. Peng, X. Shao, et al., *ACS Appl. Mater. Interfaces* 8 (2016) 19353–19363.
- [67] N. Liu, X. Zhang, N. Li, et al., *Small* 15 (2019) 1907.
- [68] S. Lin, Q. Zhang, S. Li, et al., *ACS Appl. Mater. Interfaces* 12 (2020) 11397–11408.
- [69] J. Zhu, M. Zhang, Y. Gao, et al., *Signal Transduct. Target. Ther.* 5 (2020) 120.
- [70] Y. Jiang, S. Li, T. Zhang, et al., *ACS Appl. Mater. Interfaces* 14 (2022) 15069–15079.
- [71] D. Zhao, M. Liu, J. Li, et al., *ACS Appl. Mater. Interfaces* 13 (2021) 29439–29449.
- [72] S. Li, Y. Liu, T. Zhang, et al., *Adv. Mater.* 34 (2022) 2204287.
- [73] X. Shao, S. Lin, Q. Peng, et al., *Small* 13 (2017) 1602770.
- [74] S. Lin, Q. Zhang, S. Li, et al., *Cell Prolif.* 55 (2022) e13279.
- [75] L. Fu, P. Li, J. Zhu, et al., *Bioact. Mater.* 9 (2022) 411–427.
- [76] X. Shao, Z. Hu, Y. Zhan, et al., *Cell Prolif.* 55 (2022) e13272.
- [77] L. Wang, Y. Wang, Y. Jiang, et al., *ACS Nano* 10 (2023) 24187–24199.
- [78] Y. Zhao, S. Li, M. Feng, et al., *Small* 19 (2023) e2302326.
- [79] L. Liu, P. Hu, Y. Liu, et al., *ACS Appl. Mater. Interfaces* 15 (2023) 25403–25416.
- [80] X. Yu, Y. Wang, L. Ran, et al., *Nano Lett.* 23 (2023) 8816–8826.
- [81] Y. Wang, W. Jia, J. Zhu, et al., *Chin. Chem. Lett.* 34 (2023) 107746.
- [82] J. He, W. Chen, X. Chen, et al., *Cell Prolif.* 56 (2023) e13495.
- [83] X. Yang, F. Zhang, Y. Du, et al., *Chin. Chem. Lett.* 33 (2022) 1901–1906.
- [84] Y. Liu, S. Li, S. Lin, et al., *Chin. Chem. Lett.* 34 (2023) 107987.
- [85] X. Chen, J. He, Y. Xie, *Cell Prolif.* 56 (2023) e13424.
- [86] W. Cui, Y. Zhan, X. Shao, et al., *ACS Appl. Mater. Interfaces* 11 (2019) 32787–32797.
- [87] Y. Yao, Y. Wen, Y. Li, et al., *Nanoscale* 13 (2021) 15598–15610.
- [88] M. Zhou, T. Zhang, X. Zhang, et al., *ACS Appl. Mater. Interfaces* 14 (2022) 37478–37492.
- [89] J. Li, Y. Yao, Y. Wang, et al., *Adv. Mater.* 34 (2022) 2202513.
- [90] J. Zhu, Y. Yang, W. Ma, et al., *Nano Lett.* 22 (2022) 2381–2390.
- [91] W. Ma, Y. Zhan, Y. Zhang, et al., *ACS Appl. Mater. Interfaces* 12 (2020) 2095–2106.
- [92] T. Zhang, M. Zhou, D. Xiao, et al., *Adv. Sci.* 9 (2022) e2202058.
- [93] X. Qin, L. Xiao, N. Li, et al., *Bioact. Mater.* 14 (2022) 134–144.
- [94] X. Qin, B. Zhang, X. Sun, et al., *ACS Appl. Mater. Interfaces* 15 (2023) 7793–7803.
- [95] S. Gao, Y. Li, D. Xiao, et al., *Nano Lett.* 21 (2021) 4437–4446.
- [96] Z. Cai, Y. Li, L. Bai, et al., *ACS Nano* 17 (2023) 22668–22683.
- [97] X. Liu, Z. Yu, Y. Wu, et al., *Cell Prolif.* 54 (2021) e13084.
- [98] S. Gao, Y. Wang, Y. Li, et al., *ACS Appl. Mater. Interfaces* 13 (2021) 42543–42553.
- [99] W. Wang, D. Xiao, L. Lin, et al., *Adv. Healthc. Mater.* 12 (2023) e2203076.
- [100] R. Yan, W. Cui, W. Ma, et al., *ACS Nano* 17 (2023) 8767–8781.
- [101] Y. Chen, S. Shi, B. Li, et al., *ACS Appl. Mater. Interfaces* 14 (2022) 13136–13146.
- [102] T. Tian, C. Zhao, S. Li, et al., *ACS Appl. Mater. Interfaces* 15 (2023) 10492–10505.
- [103] W. Fu, C. You, L. Ma, et al., *ACS Appl. Mater. Interfaces* 11 (2019) 39525–39533.
- [104] S. Shi, W. Fu, S. Lin, et al., *Nanomedicine* 21 (2019) 102061.
- [105] G. Song, H. Dong, D. Ma, et al., *ACS Appl. Mater. Interfaces* 13 (2021) 46334–46342.
- [106] D. Song, Y. Cheng, X. Li, et al., *ACS Appl. Mater. Interfaces* 9 (2017) 14724–14740.
- [107] W. Durante, *Curr. Drug Targets* 11 (2010) 1504–1516.
- [108] M. Zhang, J. Zhu, X. Qin, et al., *ACS Appl. Mater. Interfaces* 11 (2019) 30631–30639.
- [109] Q. Chen, F. Ding, S. Zhang, et al., *Nano Lett.* 21 (2021) 4394–4402.
- [110] M. Zhou, S. Gao, X. Zhang, et al., *Bioact. Mater.* 6 (2021) 1676–1688.
- [111] A. El-Remessy, M. Coucha, S. Elshaer, W. Eldahshan, B. Mysona, *Middle East Afr. J. Ophthalmol.* 22 (2015) 135.
- [112] X. Zhang, M. Zhang, M. Zhou, et al., *ACS Appl. Mater. Interfaces* 14 (2022) 6442–6452.